PREPARATION AND CHARACTERIZATION OF CELLULOSE DIACETATE DERIVED MODIFIED MAGNETIC BIOCHAR FOR REMOVAL OF CHROMIUM(VI) IONS FROM AQUEOUS SOLUTION

May Thazin Kyaw[1], Aung Than Htwe[2]

Abstract

Biochar (BC) derived from peanut hulls is a potential low-cost adsorbent for metal ions and organic pollutants, but its practical application is still limited by the adsorption capacity. In this study, cellulose diacetate (CDA) was prepared from waste cigarette filters by solution casting method. A cellulose diacetate magnetic biochar (CDMBC) and cellulose diacetate biochar (CDBC) were synthesized through chemical co-precipitation, with cellulose diacetate from prepared magnetic biochar (MBC) and biochar (BC). The morphologies, surface chemical structures, and crystallinity of the prepared BC, MBC, CDBC and CDMBC were characterized by SEM, XRD, TG-DTA, and FT IR. The adsorption of Cr(VI) ions by using different biochars as adsorbents was investigated under different adsorption conditions. Batch experiments were conducted to investigate the effect of metal concentrations, adsorbent dosage, time and pH values on the adsorption of Cr(VI). The Freundlich and Langmuir isotherm models were utilized in the analysis of experimental results to determine the optimal fit for the adsorption process of Cr(VI). CDMBC biochar showed the highest removal efficiency of Cr(VI) ions, attributed to enhanced surface area, active sites, and improved magnetic properties. In this research, the cellulose diacetate derived magnetic biochar could be used to remove the Cr(VI) ions in the environmental pollution of Cr(VI) contaminated waste water.

Keywords: biochar, cellulose diacetate, magnetic biochar, isotherm models, adsorption

Introduction

The rapid development of modern industry, has caused most industrial wastewater to contain toxic metals or other ions that affect environmental pollution and endanger human health. Heavy metal ions such as copper, cadmium, chromium, lead and mercury ions are highly dangerous to human beings as well as the environment, even at low concentration levels in water. These heavy metal ions tend to accumulate in the tissues of living organisms, whether in plants or animals, and cause many problems such as inhibiting natural growth and changes in the structure and function of cells resulting in disease and even cell death. For this reason, the treatment of toxic heavy metal ion pollution in water has received and extensive concern (Cao *et al*., 2010).

Chromium is used in electroplating, leather, textile, and tanning industries, and these industries discharge chromium-rich effluents into the nearby waterbodies, thus contaminating the environment (Saravanan *et al*. 2017). In aqueous media, chromium exists in two forms: Cr (III) and Cr (VI). The oxidation number of chromium depends on the pH value of the aqueous medium, and changing the pH can change chromium from one form to another (Sharma *et al*. 2008).

[1] Department of Chemistry, University of Yangon
[2] Department of Chemistry, University of Yangon

The toxicity of chromium for humans is dependent on the exposure duration and dose, and it has been found that hexavalent chromium is more toxic than trivalent. Long-term exposure to chromium can damage the skin, eyes, blood, immune system, and respiratory system (Zhang *et al.* 2014). Chromium also damages DNA, creates oxidative stress, and can cause the development of tumors in the human body (Mishra *et al.* 2016). Various methods have been reported for the removal of chromium and various adsorbents have been employed for the elimination of heavy metals from wastewater (Wu *et al*, 2013).

The aim of this study is to prepare cellulose diacetate derived waste cigarette filters modified magnetic biochar for removal of Cr(VI) ions from aqueous solution. The prepared cellulose diacetate modified magnetic biochar were characterized using SEM, XRD, FTIR, TG-DTA and UV-Vis. The effect of loading samples, contact time, solution pH, adsorbent dosage, temperature and initial Cr(VI) concentration as well as the adsorption isotherm of Cr(VI) on prepared cellulose acetate modified magnetic biochar were investigated in batch experiments.

Materials and Methods

Waste cigarettes and peanut hulls were collected from domestic waste. Glycerol, and potassium dichromate were purchased from the British Drug House (BDH) Chemical Ltd, England. Chemicals such as glacial acetic acid, and ferric chloride were purchased from Merck, Indonesia. All of the chemicals used in this study were of analytical grade. In all investigations, the recommended standard methods and techniques involving both conventional and modern methods were used.

Preparation of Cellulose Diacetate (CDA)

The CDA were prepared via a solution casting method. Firstly, collected waste cigarette filters were washed with ethanol and hot water several times and then were dried at 60 °C. Secondly, the above waste cigarette filters were dissolved in glacial acetic acid at the ratio of 1:15 (w/w), and then were treated using an overhead stirrer for 4 h to form a homogeneous emulsion.

Synthesis of Biochar (BC) and Magnetic Biochar (MBC)

Peanut hulls were washed with water and dried in an oven at 70°C for 9 h. The purified peanut hull powder was placed in a crucible and heated at 250°C in the muffle furnace for 1h, followed by washing with 0.1 M sulphuric acid (H_2SO_4) to remove the ash powder and washing with distilled water. Finally, the neutralized char powder was dried in oven at 70°C for 24 h. The biochar sample obtained was coded as BC. For magnetic biochar (MBC), the grounded peanut hull was soaked in 2M ferric chloride ($FeCl_3$) solution 1:8 (w/v), and then treated using an overhead stirrer for 1 h with heat at 60°C for 30 min. The hot solution was filtered, and the residue was dried in an oven at 70°C for 24 h. The residue was washed with water several times, and then the residue was placed into the muffle furnace at 600°C for 2 h (Zhang and Mao, 2013). Figure 1 shows the diagram for preparation of biochar and magnetic biochar from peanut hull.

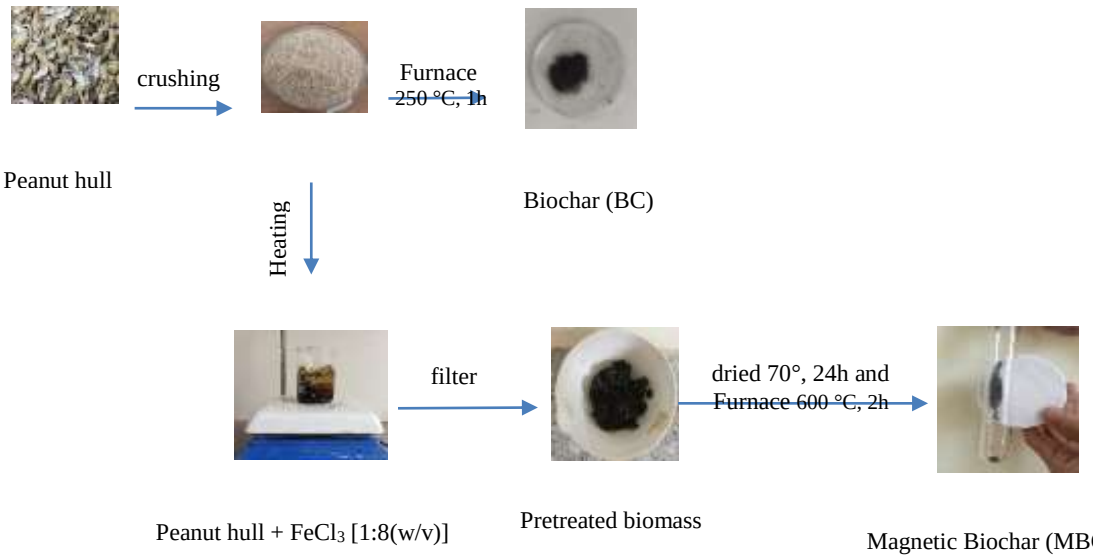

Figure 1. A diagram for preparation of biochar (BC) and magnetic biochar (MBC) from peanut hull

Synthesis of Cellulose Diacetate Coated Biochar (CDBC) and Magnetic Biochar (CDMBC)

Firstly, 1 g each of BC and MBC was mixed with the 3% cellulose diacetate (CDA) solution and stirred for 30 min to form a homogenous solution. Secondly, that solution was made into a bead by dropping it into 450 mL of 1M NaOH solution. And then the beads were placed in NaOH solution for overnight, filtered, and washed with ethanol followed by water. In the next step, the beads were dried in oven at 70°C for 2 h and ground with a motor and pestle. Figure 2 shows the preparation diagram of cellulose diacetate biochar (CDBC) and cellulose diacetate magnetic biochar (CDMBC) from peanut hull.

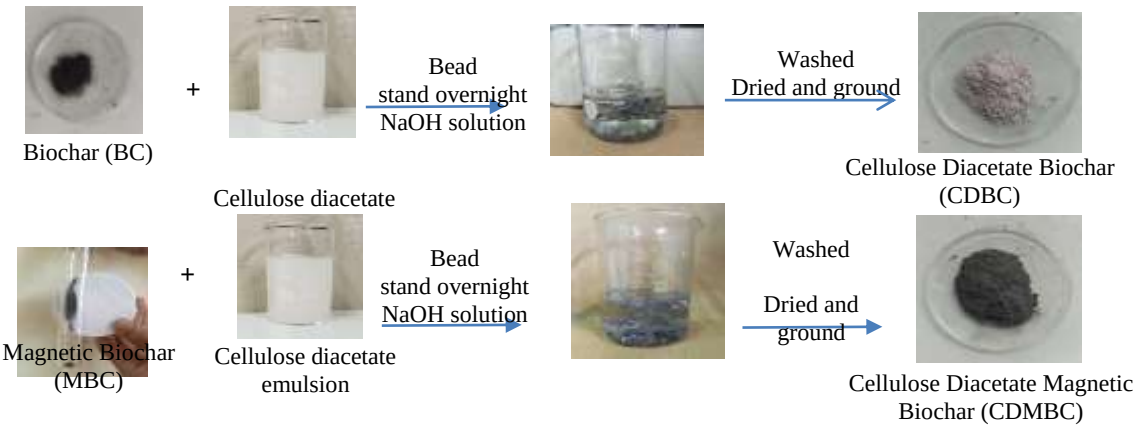

Figure 2. A diagram for preparation of cellulose diacetate biochar (CDBC) and cellulose diacetate magnetic biochar (CDMBC) from peanut hull

Characterization

The surface morphology of different biochars was studied using SEM (JOE-JSM-5610 LV model, Japan). SEM images of samples were collected under an accelerating voltage of 5 kV. Fourier transform infrared spectrophotometer (Shimadzu, Japan) was used. The resolution was 4 cm^{-1} with 64-time scanning, in the range of 4000–400 cm^{-1}. The X-ray diffraction (XRD) measurements of the different biochars were recorded using the Shimadzu 8000 X-ray diffractometer (Shimadzu, Japan) with a detector operating under a voltage of 40.0 kV and a current of 30.0 mA using Cu Kα radiation (λ = 0.15418 nm). The recorded range of 2θ was 5–40°, and the scanning speed was 6°/min. The thermal properties of different biochars were characterized by thermogravimetric analysis (TGA) on a thermogravimetric analyzer (Rigaku Thermoplus TG 8120) in the range of 30-600°C at a heating rate of 10°C min^{-1} under N_2 flow.

Batch Adsorption Experiment

Batch equilibrium tests were carried out for the adsorption of Cr^{6+} on different sample adsorbents. The samples (BC, CDBC, MBC, CDMBC) of certain doses were introduced into the 250 mL conical flasks containing 20 mL of Cr^{6+} solution of decided concentration and pH value, respectively (Ma *et al*. 2016). The flasks were then placed on a shaker and shaken with a stirring speed of 200 rpm for 2 h~~ours~~ until adsorption equilibrium was obtained. During the experiment, the initial pH 1 to 8 value of the solutions was adjusted by adding either 0.1 M HCl or 0.1 M NaOH solution before the adsorption experiment (Liu *et al*. 2010). The adsorption capacity q_e (mg/g) was calculated by Eq 1. (Chen *et al*. 2012), and the removal rate W (%) of heavy metals calculated from the following Eq. 2,

$$q_e = \frac{(C_i - C_e)V}{M} \quad (1)$$

$$\% \text{ removal (W)} = \frac{C_i - C_e}{C_i} \times 100\ \% \quad (2)$$

Where, C_i is the initial concentration of chromium ions and C_e is the equilibrium or final concentration of chromium ions, V is the volume of aqueous solution (mL), and M is the weight (g) of sample produced.

Results and Discussion

Scanning electron microscopy (SEM) Analysis

The surface morphology of the prepared BC, MBC, CDBC and CDMBC is shown in Figure 3. The SEM images in Figures 3(a) and (b) indicate that the structure of biochar (BC), possessed a more porous and rougher than that of MBC. In addition, a distinct change was found in the image of MBC which has small iron oxide particles loaded on the biochar surface. As seen in Figures 3(c) and (d), CDBC shows a flat-like structure, whereas CDMBC possesses more aggregate with small iron particles in the surface.

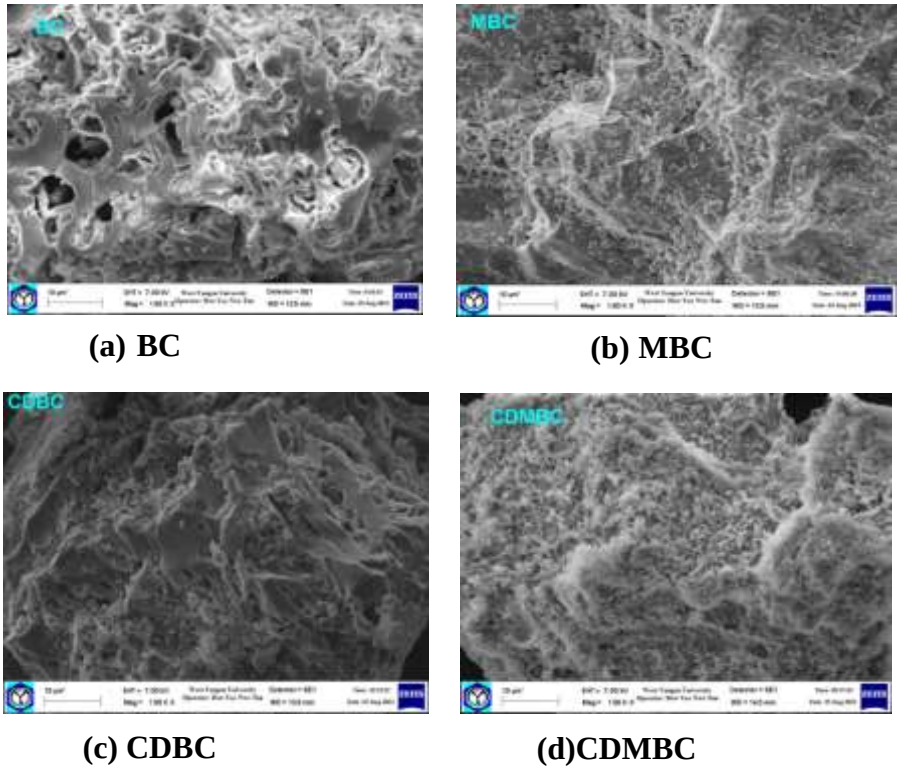

(a) BC **(b) MBC**

(c) CDBC **(d)CDMBC**

Figure 3. SEM images of (a)BC, (b) MBC, (c) CDBC, and (d) CDMBC

X-ray diffraction analysis

The XRD analysis of BC, MBC, CDBC, and CDMBC are shown in Figure 4. The diffractogram indicates the more or less amorphous by the blend with graphitization. If it is totally amorphous wood charcoal or biochar, the 2θ value will be about 20° and only a big hump will be observed. The diffractograms of all samples are observed to show the same pattern as each other. The graph indicates that BC and CDBC had a graphite crystal structure with the diffraction peaks at 21.85° and 23.45° In the XRD patterns of MBC and CDMBC, the new peaks appeared at 21.61° and 35.51° were assigned as γ-Fe_2O_3 and Fe_3O_4, respectively. These results further confirmed that iron oxide particles were successfully loaded onto cellulose diacetate and γ-Fe_2O_3 particle-containing biochar formed (Hong *et al.*, 2019). From the diffractograms, it was found that all samples show amorphous nature, which is supported to better sorption behavior for BC, MBC, CDBC, and CDMBC samples.

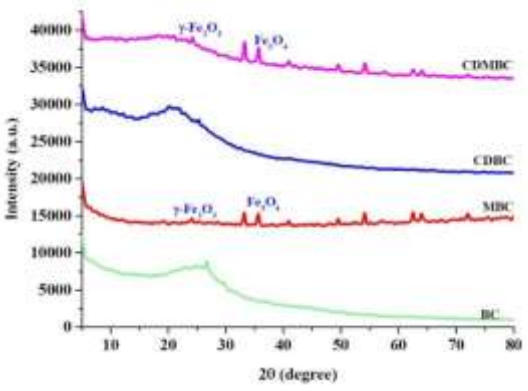

Figure 4. XRD diffratograms of (a)BC, (b) MBC, (c) CDBC, and (d) CDMBC

FT IR Spectroscopy

The FT IR spectra and spectroscopic assignment of BC, MBC, CDBC, and CDMBC are shown in Figure 5. The most characteristic peaks for CD are 3460 cm^{-1} corresponding to OH group, 2930 cm^{-1} attributed to asymmetric and symmetric C-H stretching, 1758 cm^{-1} due to carbonyl -C=O of COOR group, 1377 cm^{-1} resulted from methyl group and 1060 $cm^{-1}$for cyclic ether bonds (Gulec *et al.,* 2010). In addition, BC and MBC, a broad peak at approximately 3464 cm^{-1} were assigned the stretching of the O–H group. The peak around 1629 cm^{-1} was attributed to C=C stretching vibration of an aromatic ring. The characteristic bands at 1062 cm^{-1} involve the stretching vibration of C–O esters and ethers. The FT IR spectrum of MBC exhibited three new peaks at 2345 cm^{-1}, 2356 cm^{-1} and 2369 cm^{-1} in comparison with BC and CDBC. Moreover, the peaks at 1629 cm^{-1} became stronger, while the peak at 1062 cm^{-1} was weaker than that in BC. This is due to the effect of the iron presence in the surfaces of MBC and CDMBC. In MBC and CDMBC, there were new peaks at 495 cm^{-1}, 563 cm^{-1}, and 612 cm^{-1}, due to Fe–O, testifying to the formation of iron oxides (Fe_3O_4) (Hoang *et al*., 2019). These results further ascertained that iron was successfully loaded onto biochar and led to an increase in the amount of surface functional groups of MBC and CDMBC. These functional groups enhance adsorption through hydrogen bonding and complexation with metal ions (Tan *et al*., 2017). This can be an important factor to enhance the Cr(VI) adsorption onto MBC and CDMBC from aqueous solution.

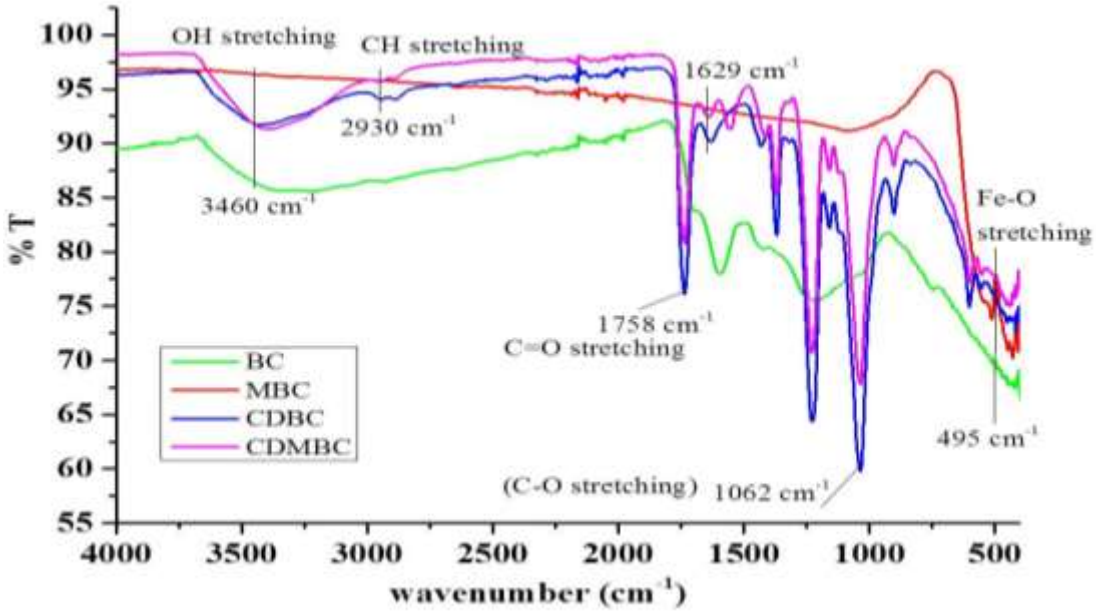

Figure 5. FT IR spectra of BC, CDBC, MBC, CDMBC

TG-DTA analysis

Thermogravimetric analysis was performed to evaluate the thermal stability of materials as well as to confirm the amount of BC, CDBC, MBC and CDMBC. The thermograms of BC, MBC, CDBC and CDMBC show the (a)thermogravimetry (TG) curves and (b) differential thermal analysis (DTA) curves (Figure 6). According to the TG thermogram profiles, BC showed three decomposition stages with weight loss of 10.83% at a temperature range of 38.86 °C to 280.97 °C, 29.68% at a temperature range of 280.97 °C to 433.02 °C, and 55.36% at a

temperature range of 433.02 °C to 600 °C, respectively. The process involves firstly the removal of water (endothermic peak at 78.4 °C) and light volatile components; secondly, the degradation of hemicellulose (exothermic peak at 338.7 °C); and lastly, the decomposition of lignin and cellulose (exothermic peak at 478.73 °C) in three stages. CDBC also showed three decomposition stages with weight losses of 7.22 %, 60.82 % and 29.39%, respectively. These stages were attributed to the loss of surface water followed by the combustion of polymer materials. CDMBC showed three decomposition stages with weight losses of 6.62%, 50.67% and 7.07%, respectively.

It can be seen that the mass losses at around 750 °C could be the reduction of magnetite Fe^{3+} to Fe^{2+} by the following reactions (1) and (2). Thus, it agrees with the observation of the Fe–O bond in the FTIR spectra.

$C_nH_nO \rightarrow$ C + volatiles (CO_x, H_2O, organics) (1)

$2Fe_3O_4 + C \rightarrow 6FeO + CO_2$ (2)

TGA results also demonstrated that the MBC exhibited more thermally stable than the original biochar. This is due to the activation effect during pyrolysis observed by adding the $FeCl_3$ to the biomass (Htwe *et al*., 2022).

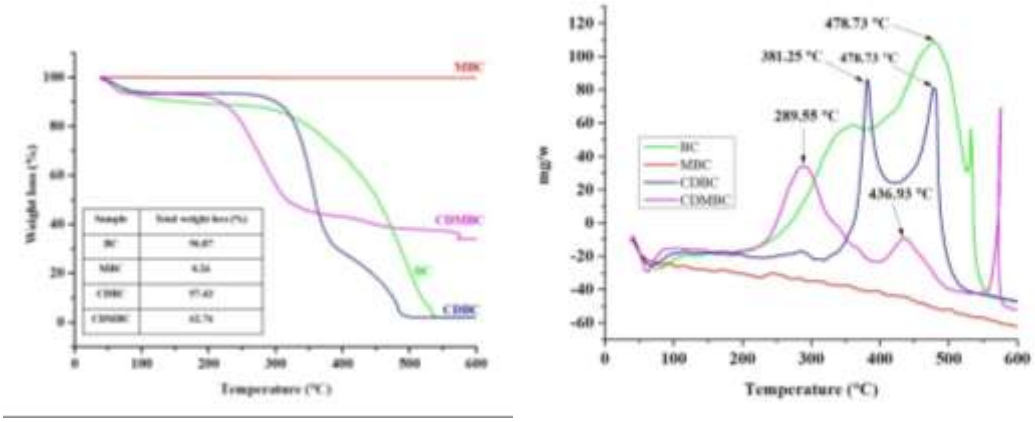

Figure 6. (a) TG curves and (b) DTA curves for BC, MBC, CDBC and CDMBC

UV-Vis absorption spectra

The UV-vis spectrum (Figure 7) of BC and MBC showed a single peak at around 216 nm. The CDBC and CDMBC peaks show at 227 nm. It was found that the intensity of BC and MBC is lower than that of CDBC and CDMBC. According to this figure, cellulose diacetate coated magnetic biochar change in the UV–vis spectra, and this confirms the binding of cellulose diacetate binding magnetic biochar.

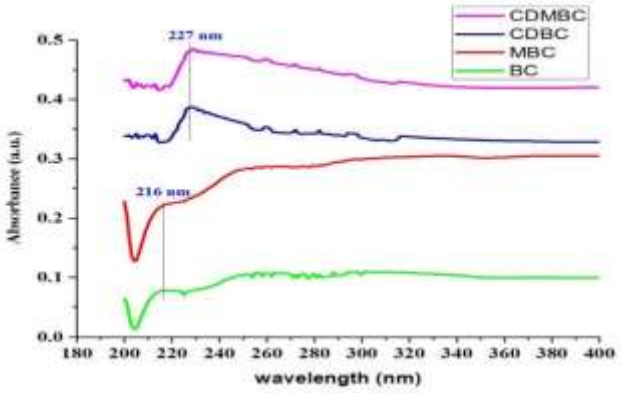

Figure 7. UV-vis spectra for BC, MBC, CDBC and CDMBC

Adsorption performances of Cr(VI) ion with BC, MBC, CDBC and CDMBC

Effect of solution pH

The pH plays a crucial role in the determination of the ionization degree and the surface properties of the adsorbents. The solution pH ranged from 3-8 for an initial metal ion concentration of 100 ppm, was determined by a UV-Visible spectrophotometer at 540 nm (Figure 8). At pH 5, the maximum removal efficiencies were observed, with CDMBC achieving the highest removal rate of 76.50%. Below pH 6, Cr(VI) exists as $HCrO^{4-}$ and $Cr_2O_7^{2-}$, which interact strongly with the positively charged adsorbent surface. As pH increases from 6 to 8, the OH–ions dominate, reducing adsorption due to competition for active sites and decreased surface protonation. Magnetic biochar (MBC) and cellulose diacetate magnetic biochar (CDMBC) consistently outperformed other samples, showcasing enhanced removal rates at acidic pH levels (Hoang *et al.*, 2019).

The higher efficiency of MBC and CDMBC is attributed to their increased surface functionality and charge density. These biochar demonstrated better performance across varying dosages (0.1–0.5 g), with adsorption efficiency slightly decreasing due to site saturation at higher dosages. The Cr(VI) adsorption mechanism involves the electrostatic attraction at lower pH and ion exchange at higher pH. These findings suggest that modified biochars are particularly effective for Cr(VI) removal, especially at lower pH levels where adsorption is more favorable. This highlights their potential for practical applications in treating Cr(VI)-contaminated water (Inyang *et al.*, 2012)..

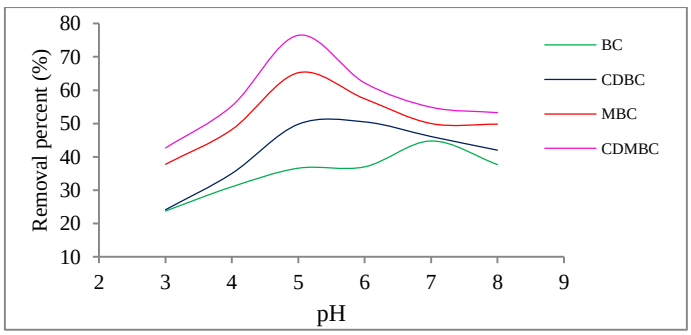

Figure 8. Effect of pH of BC, CDBC, MBC CDMBC on adsorption of Cr^{6+} ions (condition: dosage of 0.1 g; initial concentration of 100 ppm; volume of 25 mL, contact time of 3 h, temperature of 25 °C)

Effect of Initial Concentration of Cr^{6+} ion

The effect of initial concentration on the Cr(VI) removal by BC, MBC, CDBC and CDMBC is shown in Figure 9. The removal efficiency of 35.0 % found to be decreased with the initial concentration of Cr(VI) increasing from 100 to 500 mg/L. Apparently, an adsorbent with a certain mass had a limited number of active sites and these sites progressively approached saturation as the Cr(VI) concentration increased. Thus, the saturated adsorbent cannot adsorb more Cr(VI) ions, which resulted in a decrease in removal efficiency in high concentration of Cr(VI).

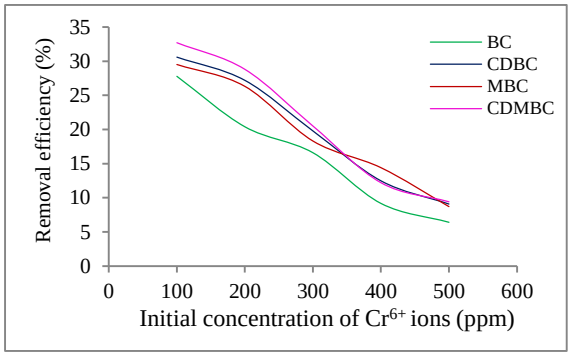

Figure 9. Effect of initial concentration of BC, CDBC, MBC CDMBC on adsorption of Cr^{6+} ions (condition: dosage of 0.1g; pH 5; volume of 25 mL, contact time of 3 h, temperature of 25 °C)

Effect of Dosage

This study, investigate the effect of adsorbent amount on 100 ppm Cr(VI) solution in varying adsorbent dosages (0.1-0.5 g) as shown in Figure 10. As the dosage increased, the removal efficiency improved particularly for BC and CDMBC, indicating that the availability of more adsorption sites facilitates enhanced the ions capture. However, beyond a certain dosage (0.3 g), the removal rate plateaued, due to the aggregation of biochar particles at higher dosages, reducing the effective surface area and active sites accessible for Cr(VI). CDMBC maintained a consistently higher removal efficiency, making it a cost-effective option for large-scale applications (Bandaru *et al*., 2013).

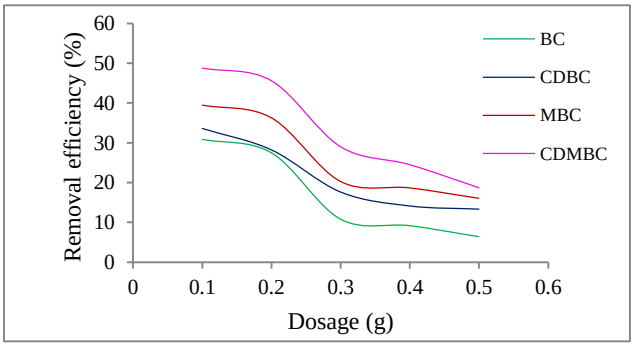

Figure 10. Effect of dosage of BC, CDBC, MBC CDMBC on adsorption of Cr^{6+} ions (condition: initial concentration 100 ppm; pH 5; volume of 25 mL, contact time of 3 h, temperature of 25 °C)

Effect of Time

This study investigated the effect of contact time on 100 ppm Cr (VI) solution at pH 5 with 0.1 g adsorbent for varying time intervals at temperature 25 °C (Figure 11). Rapid adsorption round about 33.2 % removal efficiency occurred in the first three hours and peaked for the majority of adsorbents, such as MBC and CDBC, as the contact period increased from one to five hours.

After 3 h, the adsorption process reaches equilibrium, with the removal rates either leveling off or decreasing, was observed in BC. This initial rapid adsorption can be attributed to the availability of abundant active sites on the adsorbents surface, facilitating quick Cr(VI) ion binding. The drop in removal efficiency for BC beyond 3 h may be due to desorption or competition between Cr (VI) ions and other ions present in the solution (Jain *et al*., 2010) Therefore, an optimal contact time of around 3 h is optimized for maximum Cr (VI) removal.

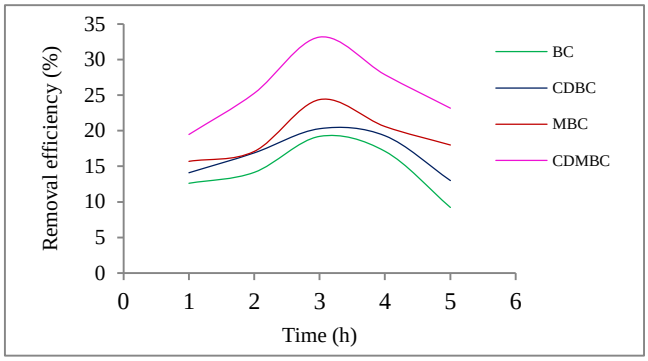

Figure 11. Effect of contact time of BC, CDBC, MBC CDMBC on adsorption of Cr^{6+} ions (condition: initial concentration 100 ppm; pH 5; volume of 25 mL, dosage of 0.1 g, temperature of 25 °C)

Effect of Temperature

The results indicate that the removal efficiency of Cr (VI) varies with temperature for all samples (Figure 12). For BC, the removal percentage peaks at 30 °C with approximately 99.3 % efficiency, then decreases slightly before increasing again at 40 °C. This suggests that higher temperatures enhance the kinetic energy of the ions, promoting interaction with the active adsorption sites on the biochar surfaces. In contrast, MBC and CDMBC exhibit more stable removal efficiencies across all temperature, suggesting that their adsorption processes are less temperature sensitive. The decreased removal rates at higher temperatures for CDBC, could be due to the weakening of physical adsorption forces and possible desorption of Cr (VI) ions (Foo and Hameed, 2010). Thus, 30 °C is optimal for the maximum removal efficiency of BC, while other adsorbents show more stability across the tested temperature range.

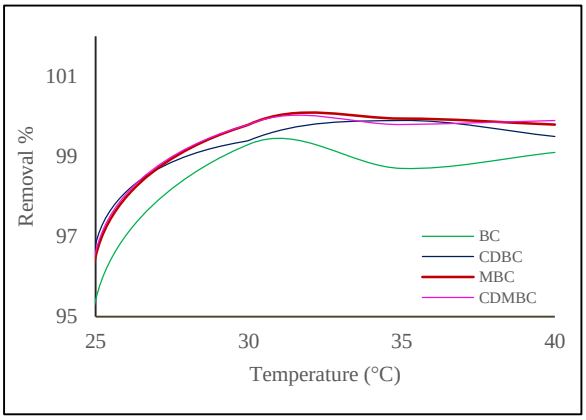

Figure 12. Effect of temperature of BC, CDBC, MBC CDMBC on adsorption of Cr^{6+} ions (condition: initial concentration 100 ppm; pH 5; volume of 25 mL, dosage of 0.1 g, contact time of 3 h)

Isotherm Modeling

The sorption isotherms were generated by varying the ratio of sorbate. Langmuir and Freundlich models were used to simulate the adsorption isotherms of Cr (VI) to the BC, CDBC, MBC and CDMBC.

Langmuir: $\frac{1}{q_e} = \frac{1}{q_m K_L C_e} + \frac{1}{q_m}$ (Langmuir, 1918)

Freundlish: $\log q_e = \log K_F + \frac{1}{n} \text{Log } C_e$ (Freundlish, 1906)

Where q_e is the amount of adsorbate adsorbed per unit mass of adsorbent at equilibrium (mg/g), C_e is the equilibrium concentration of the adsorbate in the solution (mg/L), q_m is the maximum adsorption capacity (mg/g), K_L is the Langmuir constant related to the affinity of the binding of the binding sites (L/g), K_F is the Freundlish constant, and n is the Freundlish constant indicative of the adsorption intensity or surface heterogeneity.

Table 1. Langmuir and Freundlish Isotherm Constants for Cr(VI) Adsorption onto BC, CDBC, MBC, CDMBC

Isotherm Model	Parameters	BC	CDBC	MBC	CDMBC
	q_m (mg/g)	83	23.26	8.93	2.13
Langmuir	K_L (L/g)	0.045	2.18	0.5	1.74
	R^2	0.98	0.89	0.81	0.88
	K_F	5.6	4.9	7.67	1.51
Freundlish	n	-5.32	-6.7	-5.46	-11.1
	R^2	0.88	0.85	0.86	0.94

Table 1 shows the Langmuir and Freundlish isotherm constants for Cr (VI) adsorption onto different biochar samples: BC, CDBC, MBC, and CDMBC. In the Langmuir model, the maximum adsorption capacity q_m is the highest for BC at 83 mg/g, indicating that it has the most adsorption sites available for Cr (VI). The q_m values for CDBC, MBC, and CDMBC are 23.6,

8,93, and 2.13 mg/g respectively. The Langmuir constant K_L is the highest for CDBC at 2.18 L/g, suggesting a strong affinity between Cr(VI) and the adsorption sites (Wang and Peng, 2010). The K_L values for BC, MBC and CDMBC are 0.045, 0.5 and 1.74 L/g respectively. The R^2 values close to 1 for all samples indicate that the Langmuir model fits the adsorption data well (Foo and Hameed, 2010). In the Freundlish isotherm model. the K_F value, indicative of adsorption capacity, is the highest for MBC (7.67) followed by BC (5.6), CDBC (4.9) and CDMBC (1.51). The negative (n) values suggest a non-ideal adsorption process, possibly due to heterogeneous surface conditions. The R^2 values for the Freundlish model also suggest a good fit to the experimental data (Yang, 2003). Overall, BC exhibits the highest adsorption capacity for Cr (VI), making it the most effective adsorbent among the samples tested. This suggests that the unmodified biochar sites is suitable for Cr(VI) adsorption compared to the modified versions.

Conclusion

This study demonstrated the synthesis and application of various biochars, including biochar (BC), magnetic biochar (MBC), cellulose diacetate biochar (CDBC), and cellulose diacetate magnetic biochar (CDMBC), for the adsorption of Cr (VI) ions from aqueous solutions. The characterization techniques such as SEM, XRD, FT IR, and TG DTA provided insights into the structural and chemical properties of the synthesized biochars. The adsorption experiments revealed that the removal efficiency of Cr (VI) ions was significantly influenced by parameters such as initial metal ion concentration, pH, and adsorbent dosage. Among the biochars studied, CDMBC exhibited the highest removal efficiency for Cr (VI) ions, particularly at lower pH levels and higher dosages. This performance can be attributed to the enhanced surface area, increased active sites, and improved magnetic properties provided by the cellulose diacetate coating and the magnetic modification. The maximum adsorption capacities (q_m) derived from the Langmuir isotherm model were the highest for BC, followed by CDBC, MBC, and CDMBC. The Langmuir constant (K_L) values suggested a strong affinity between Cr (VI) ions and the adsorption sites, particularly for CDBC. The Freundlich isotherm model also supported the high adsorption capacity and intensity, especially for MBC. The Langmuir and Freundlich isotherm models are in good agreement with the adsorption results of Cr (VI) ions onto the biochars.

Overall, this study highlights the potential of using waste-derived biochars, particularly CDMBC, as cost-effective and efficient adsorbents for the removal of toxic Cr(VI) ions from wastewater. These findings suggest that CDMBC could be a promising material for managing industrial effluents and protecting water resources from heavy metal contamination.

Acknowledgements

The authors owe their gratitude to Professor Dr. Ni Ni Than, Head of Department, Department of Chemistry, University of Yangon, Yangon, Myanmar, for her stimulating suggestion for MAAS.

References

Ahmad, M., S.S. Lee, X. Dou, D. Mohan, J.K. Sung, J.E. Yang, and Y.S. Ok. (2012). "Effects of Pyrolysis Temperature on Soy bean Stover-and Peanut Shell-derived Biochar Properties and TCE Adsorption in Water". *Bioresource Technology*, vol.118, pp.536-554.

Bandaru, N.M., N. Reta, H. Dalal, A.V. Ellis, J. Shapter and N.H. Voelcker. (2013). "Enhanced Adsorption of Mercury Ions on Thiol Derivatized Single Wall Carbon Nanotubes". *Journal of Hazardous Materials*, vol. 261, pp. 534-541.

Cao, J., Y. Tan, Y. Che, and H. Xin. (2010). "Novel Complex Gel Beads Composed of Hydrolyzed Polyacrylamide and Chitosan: An Effective Adsorbent for The Removal of Heavy Metal from Aqueous Solution". *Bioresource. Technol*, vol. 101, pp.2558-2561.

Chen, J. H., J.C. Ni, L.Q. Liu, and S.X. Li. (2012). "Adsorption Behavior of Cd (II) Ions on Humic Acid-Immobilized Sodium Alginate and Hydroxyethyl Cellulose Blending Porous Composite Membrane Adsorbent". *Desalination* vol.285(3), pp. 54-61.

Foo, K.Y. and B.H. Hameed. (2010). "Insights into the Modeling of Adsorption Isotherm Systems". *Chemical Engineering Journal*, vol.156 (1), pp.2-10.

Freundlish, H. (1906). "Over the Adsorption in Solution". *International Journal of Research in Physical Chemistry and Chemical Physics*,vol. 57, pp. 387-470.

Gulec H., A. Topacli, C.F. Topacli, N. Albayrak, and M. Mutlu. (2010). "Modification of Cellulose Acetate Membrane via Low-pressure Plasma Polymerization for Sugar Separation Applications: part I. Membrane Development and Characterization", *J. Membrane Sci.*, vol.350, pp. 310–321.

Hoang L. P., H. T. Van, L. H. Nguyen, D. Mac, T. T. Vu, L. T. Ha and X. C. Nguyen. (2019). "Removal of Cr(VI) from Aqueous Solution using Magnetic Modified Biochar Derived from Raw Corncob", *New J. Chem.*, vol.43, pp.18663-18672

Htwe, A.T., M.T.M. Maung, and Z. Naing. (2022). "Synthesis of Chitosan-coated Magnetite Nanoparticles using Co-precipitation Method for Copper (II) ions Removal in Aqueous Solution". *World Journal of Engineering*, vol. 19 (5), pp.726-734

Inyang, M., B. Gao, Y. Yao. Y. Xue, A. R. Zimmerman, P. Pullammanappallil and X, Cao. (2012). "Removal of Heavy Metals from Aqueous Solution by Biochars Derived from Anaerobically Digested Biomass". *Bioresource Technology*, vol.110, pp. 50-56.

Jain, M., V.K. Garg, and K. Kadirvelu. (2010). "Chromium Removal from Aqueous System using Helianthus Annuus (Sunflower) Stem Waste". *Journal of Hazardous Materials*. vol. 173 (1-3). pp. 448-454.

Langmuir, I. (1918). "The Adsorption of Gases on Plane Surfaces of Glass, Mica and Platinum". *J. Am. Chem. Soc*, vol.40, pp. 1361-1403.

Lin, S.H., R.S. Jaung. (2009). "Adsorption of Phenol and Its Derivatives from Water using Synthetic Resins and Low-Cost Natural Adsorbents". *J. Environ. Manag*. vol.90, pp. 1336-1349.

Liu, J., Y. Ma, T. Xu, and G. Shao. (2010). "Preparation of Zwitterionic Hybrid Polymer and Its Application for the Removal of Heavy Metal Ions from Water". *J. Hazard. Mater*. vol.**178** (1-3), pp. 1021-1029.

Mishra, S., T.N. Toxic. (2016). "Genotoxic Effects of Hexavalent Chromium in Environment and its Bioremediation Strategies". *J. Environ. Sci. Health Part C,*vol. 34, pp.1-32.

Mohan, D., C.U. Pittman, and P.H. Steele. (2006). "Pyrolysis of Wood/Biomass for Bio-oil: a Critical Review". *Energy and Fuels*, vol.20 (3), pp. 848-889.

Wu, Y., H. H. Wang, C. Zhang, J. Zhang and Z. L. Zhang. (2013). "Adsorption of Hexavalent Chromium from Aqueous Solutions by Graphene Modified with Cetytrimethylammonium Bromide". *J. Colloid Interface Sci.*, vol. 394, pp. 183-191.

Saravanan, R., P.S. Kumar, and M. Yashwanthraj. (2017). "Sequestration of Cr (VI) ions from Industrial Wastewater using Waste Biomass: A review". *Desalination Water Treat.* vol.68, pp. 245-266.

Sari, A., and M. Tuzen. (2009). "Biosorption of Pb (II) and Ni (II) from Aqueous Solution by Lichen (Cladonia frucata) Biomass." *Biochemical Engineering Journal*. vol.**42** (3) pp. 194-201.

Sharma, S. K., B. Petrusevski, and G. Amy. (2008). "Chromium Removal from Water: A Review". *J. Water Supply Res. Technol. AQUA* vol. 57, pp. 541-553.

Tan, X. F., S. B. Liu, Y. G. Liu, Y. L. Gu, G. M. Zeng, X. J. Hu, X. Wang, S. H. Liu and L. H. Jiang. (2017) "Biochar as Potential Sustainable Precursors for Activated Carbon Production: Multiple Applications in Environmental Protection and Energy Storage". *Bioresource Technology*, vol. 227, pp. 359-372

Wang, S. and Y. Peng. (2010). "Natural Zeolites as Effective Adsorbents in Water and Wastewater Treatment". *Chemical Engineering Journal*, vol.156 (1), pp. 11-24.

Yang, R. T. (2003) *Adsorbents: Fundamentals and Applications*. Hoboken, John Wiley and Sons.

Zhang, R., Y. Xiang, Q. Ran, X. Deng, Y. Xiao, L. Xiang, and Z. Li. (2014). "Involvement of Calcium, Reactive Oxygen Species, and ATP in Hexavalent Chromium-Induced Damage in Red Blood Cells". *Cells. Phsysial, Biochem*, vol.**34**, pp. 1780-1791.

Zhang, W., and S. Mao. (2013). "Pb (II) and Cr (VI) Sorption by Biochar Pyrolyzed from The Municipal Wastewater Sludge Under Different Beating Conditions". *Bioresource. Technol*. vol 147, pp.545-552.